Journal of Solid State Chemistry 182 (2009) 83–88

Contents lists available at ScienceDirect

Journal of Solid State Chemistry

journal homepage: www.elsevier.com/locate/jssc

Synthesis, characterization and crystal structure of a novel Os(II)-supported tungstoarsenate $[HAsW_7O_{28}Os(dmso)_3]^{6-}$

Li-Hua Bi [a,*], Bao Li [a], Li-Xin Wu [a,*], Kui-Zhan Shao [b], Zhong-Min Su [b]

[a] *State Key Laboratory of Supramolecular Structure and Materials, College of Chemistry, Jilin University, Changchun 130012, PR China*
[b] *Faculty of Chemistry, Key Lab of Polyoxometalate Science of Ministry of Education, Institute of Functional Material Chemistry, Northeast Normal University, Changchun 130024, PR China*

ARTICLE INFO

Article history:
Received 13 August 2008
Received in revised form
16 September 2008
Accepted 2 October 2008
Available online 15 October 2008

Keywords:
Synthesis
Crystal structure
Osmium
Tungstoarsenate
Three-dimensional architecture

ABSTRACT

Reaction of tri-lacunary Keggin tungstoarsenate with osmium complex $Os(dmso)_4Cl_2$ under mild condition led to the formation of a novel Os (II)-supported tungstoarsenate $Na_5(NH_4)[HAsW_7O_{28}Os(dmso)_3]\cdot 15H_2O$ (**1a**). Single-crystal X-ray diffraction analysis shows that compound **1a** crystallizes in the monoclinic space group $P2_1/c$ (no. 14) with $a = 14.9166(12)$ Å, $b = 23.6935(19)$ Å, $c = 16.5349(14)$ Å, $\beta = 92.7950(10)^\circ$, $V = 5836.9(8)$ Å^3, $Z = 4$ with $R_1 = 0.0453$. The crystal structure reveals two features: (1) the polyanion $[HAsW_7O_{28}Os(dmso)_3]^{6-}$ (**1**) consists of a $Os(dmso)_3$ unit linked to a tungstoarsenate fragment $\{HAsW_7O_{28}\}$ via two Os–O–W bonds and one Os–O–As bond resulting in an assembly with C_s symmetry, which represents a novel mode of Os-coordination to a polyoxoanion framework; (2) 3D architecture assembled by the polyanion **1** and sodium linkers. In addition, the compound **1a** was well characterized by the multinuclear NMR (^{13}C, ^{1}H), IR spectroscopy, UV–vis spectroscopy, elemental analysis, and cyclic voltammetry (CV).

1. Introduction

Polyoxometalates (POMs) constitute an intriguing and distinctive class of metal–oxygen cluster species with an enormous structural variety and fascinating properties following the potential applications in catalysis, bio- and nanotechnology, medicine, material science, and so on [1–3]. POMs have been known about 200 years ago since the time of Berzelius [4]. However, POMs have been developed rapidly in recent years and the strong efforts are considered towards the modification and functionalization of POMs by incorporation or coordination of metal atoms or organometallic moieties to constitute novel structural types with function and properties [5–14].

The noble-metal substituted POMs have attracted increasing attention in general and Pd-, Pt-substituted POMs in particular due to excellent catalytic properties for the selective and efficient transformation of organic substrates and the oxidation of alkanes and alkenes by peroxides [15–18]. Recently, several structurally well-characterized Pd-substituted POMs have been reported, e.g., palladium(II)-substituted isopolytungstate $[Pd_2W_{10}O_{36}]^{8-}$ [19], palladium(II)-substituted tungstoantimonate(III) $[Cs_2Na(H_2O)_{10}Pd_3(\alpha\text{-}Sb^{III}W_9O_{33})_2]^{9-}$ [20], palladium(II)-substituted tungstosilicate $[Cs_2K(H_2O)_7Pd_2WO(H_2O)(A\text{-}\alpha\text{-}SiW_9O_{34})_2]^{9-}$ [21] and tungstoarsenates $[Na_2(H_2O)_2PdWO(H_2O)(\alpha\text{-}AsW_9O_{33})_2]^{10-}$, and $[Cs_2Na(H_2O)_8Pd_3(\alpha\text{-}AsW_9O_{33})_2]^{9-}$ [22]. More recently, the Pd and Pt in high oxidation states substituted POMs were also been presented, e.g., $[Pd^{IV}O(OH)WO(OH_2)(PW_9O_{34})_2]^{13-}$ [23], $[Pt^{IV}O(H_2O)(PW_9O_{34})_2]^{16-}$ [24], $[\alpha\text{-}SiPt_2^{IV}W_{10}O_{40}]^{8-}$ [25], $[H_2Pt^{IV}V_9O_{28}]^{5-}$ [26].

Another noble metal ruthenium-substituted POMs are exploited rapidly recently because of the unique redox-active nature and catalytic properties of the element ruthenium [27–29]. In the last couple of years, some researches have engaged in a large number of studies on the catalytic properties of ruthenium-containing POMs and it has been demonstrated that Ru-containing POMs have high reactivity and selectivity in the catalytic oxidation of a variety of organic substrates by O_2 and H_2O_2 [30–33]. To date, several different Ru precursors have been employed to synthesize Ru-substituted POMs, such as $RuCl_3\cdot nH_2O$, $[Ru^{II}(H_2O)_6][C_7H_7SO_3]_2$, $Ru(acac)_3$, *cis*-$Ru(dmso)_4Cl_2$, $[Ru(arene)Cl_2]_2$ (arene = benzene, *p*-cymene), etc. that has resulted in some unexpected structural class of Ru-containing POMs, e.g., $[HW_9O_{33}Ru_2^{II}(dmso)_6]^{7-}$ [34], $[Ru(dmso)_3(H_2O)XW_{11}O_{39}]^{6-}$ ($X =$ Ge, Si) [35], $[P_2W_{17}O_{61}\{Ru(C_6H_6)(H_2O)\}]^{8-}$ [36], $[\{PW_{11}O_{39}\{Ru(arene)\}\}_2\{WO_2\}]^{8-}$ [37,38], $[\{Ru(C_6H_6)(H_2O)\}\{Ru(C_6H_6)\}(\gamma\text{-}XW_{10}O_{36})]^{4-}$ ($X =$ Si, Ge) [39], $[\{Ru(C_6H_6)(H_2O)\}\{Ru(C_6H_6)\}(XW_9O_{34})]^{4-}$ ($X =$ Si, Ge) [40], etc.

However, parallel to the Pd-, Pt-, Ru-substituted POMs, the Os-supported POMs are extremely rare so far. There are very few reports on the studies of Os-containing POMs. In 2006, Su et al.

---

[*] Corresponding authors. Fax: +86 431 85193421.
E-mail addresses: bilihua@email.jlu.edu.cn (L.-H. Bi), wulx@jlu.edu.cn (L.-X. Wu).

0022-4596/$ - see front matter © 2008 Elsevier Inc. All rights reserved.
doi:10.1016/j.jssc.2008.10.005

investigated the electronic and redox properties of osmium-nitrido-functionalized POM species, $[PW_{11}O_{39}(OsN)]^{2-}$ by the DFT (density functional theory) calculations [41]; Proust et al. studied the reaction of $K_{10}[\alpha_2\text{-}P_2W_{17}O_{61}]$ or $K_{10}[\alpha_1\text{-}P_2W_{17}O_{61}]$ with $[Bu_4N][OsCl_4N]$ in a water/methanol mixture and characterized the compounds $[\alpha_2\text{-}P_2W_{17}O_{61}\{Os^{VI}N\}]^{7-}$ and $[\alpha_1\text{-}P_2W_{17}O_{61}\{OsN\}]^{7-}$ by multinuclear (^{183}W, ^{15}N) NMR, EPR, IR, and UV/Vis fingerprints [42]; Proust et al. synthesized the Os^{II} derivative of the monovacant $[\alpha\text{-}PW_{11}O_{39}]^{7-}$, $[PW_{11}O_{39}\{Os(dmso)_3(H_2O)\}]^{5-}$, and characterized this compound by ^{31}P NMR,^1H NMR, IR spectroscopies and DFT study [43]. To the best of our knowledge, there is only one report on the structurally characterized Os^{II}-supported heptamolybdate $[Os(II)(dmso)_3Mo_7O_{24}]^{4-}$ by Neumann et al. [44], in which the osmium (II) center is coordinated to three oxo-groups of the molybdenum-oxo core and to the sulfur atoms of three terminal dmso ligands. The same authors showed that the $[Os(II)(dmso)_3Mo_7O_{24}]^{4-}$ compound was active and stable catalysts for the aerobic oxidation of alcohols because the selective oxidation of alcohols to carbonyl compounds is a very important transformation in organic synthesis. However, as far as we know, the crystal structure of the Os^{II}-supported polytungstates has never been reported. Moreover, the potentially attractive catalytic properties of such species are a strong motivation to start this kind of research.

Herein, we report on the synthesis and X-ray crystal structure of a novel Os^{II}-supported tungstoarsenate and its multinuclear NMR and electrochemical properties.

2. Experimental section

2.1. Chemicals and methods

All chemicals were of high-purity grade, purchased from Aldrich and used as received without further purification. Deionised water was used throughout. $Na_8[HAsW_9O_{34}]\cdot 11H_2O$ and *cis*-$[Os(dmso)_4Cl_2]$ were synthesized according to the literature and characterized by IR spectra [45,46]. The elemental analyses of As, W, Os, and Na were carried out by means of an ICP-AES analyzer. The elemental analyses of N, S, C, and H were performed on a Perkin–Elmer 2400 CHN elemental analyzer. The IR spectrum (2% sample, in KBr) was recorded on a Thermo Nicolet NEXUS 670 FT-IR spectrometer. UV–vis absorption spectrum was obtained using a UV–VIS–NIR spectrophotometer (UV-3600). Electrochemical measurements were carried out on CHI 660C electrochemical workstation at room temperature under nitrogen atmosphere. A three electrode electrochemical cell was used with a glassy carbon electrode (GCE) as the working electrode, a platinum wire as the counter and an Ag /AgCl reference electrode.

2.2. Synthesis

A 0.1 g (0.18 mmol) sample of *cis*-$Os(dmso)_4Cl_2$ was dissolved in 20 mL of buffer solution (pH 6.0, 0.5MNaAc+0.5 MHAc) by addition of 0.5 g (0.19 mmol) of $Na_8[HAsW_9O_{34}]\cdot 11H_2O$. This solution was heated to 80 °C for 1 h and then cooled to room temperature. The solution was filtered and then 0.5 mL of 1.0 M NH_4Cl solution was added. This solution was allowed to evaporate in an open beaker at room temperature. A yellow crystalline product started to appear after a week. Evaporation was continued until the solvent approached the solid product (yield 0.35 g, 70% based on As). Anal. Calcd (found) for **1a**: Na 4.3 (4.5), Os 7.2 (7.3), W 48.8 (47.9), As 2.8 (2.8), S 3.6 (3.7), C 2.7 (2.5), H 2.0 (2.2) %.

NMR of **1a** in D_2O at 293 K: ^{13}C: δ 45.2(2C), 45.8(2C), 46.0(2C) ppm; ^1H: δ 3.28(6H), 3.35(6H), 3.45(6H) ppm. For comparison, dmso in D_2O at 293 K: ^{13}C: δ 38.8 ppm; ^1H: δ 2.6 ppm. UV–vis (λ, nm): 228, 186. IR for $Na_5(NH_4)$ $[HAsW_7O_{28}Os(dmso)_3]\cdot 15H_2O$ (**1a**): 1725(m), 1643(w) 1571(w), 1438(m), 1404(m), 1303(w), 1111(m), 1083(w), 1018(m), 966(m), 939(m), 891(s), 863(sh), 839(s), 738(m), 685(m), 523(m), and 432(m) cm^{-1}. The IR spectrum of **1a** shows the expected S–O stretching vibrations of coordinated dmso at ~1111, ~1083, and ~1018 cm^{-1}.

Table 1
Crystal data and structure refinement for $Na_5(NH_4)[HAsW_7O_{28}Os(dmso)_3]\cdot 15H_2O$ (**1a**)

Empirical formula	$As_4C_{24}H_{212}N_4Na_{20}Os_4O_{184}S_{12}W_{28}$	
Formula weight	10554.78	
Temperature	293(2) K	
Wavelength	0.71073 Å	
Crystal system	Monoclinic	
Space group	$P2_1/c$	
Unit cell dimensions	$a = 14.9166(12)$ Å	$\alpha = 90.00°$
	$b = 23.6935(19)$ Å	$\beta = 92.7950(10)°$
	$c = 16.5349(14)$ Å	$\gamma = 90.00°$
Volume	5836.9(8) Å^3	
Z	4	
Density (calculated)	3.003 Mg m^{-3}	
Absorption coefficient	16.708 mm^{-1}	
$F(0\,0\,0)$	4776	
Data/restraints/parameters	13623/12/638	
Goodness-of-fit on F^2	1.050	
Final R indices [$I > 2\text{sigma}(I)$]	$^aR1 = 0.0453$, $^bwR2 = 0.1133$	
R indices (all data)	$^aR1 = 0.0747$, $^bwR2 = 0.1247$	

[a] $R_1 = (\sum|F_o| - |F_c|)/(\sum|F_c|)$.
[b] $wR_2 = \sum[w(F_o{}^2 - F_c{}^2)^2]/\sum[w(F_o{}^2)^2]^{1/2}$.

Table 2
Selected bond lengths [Å] and angles [°] for $Na_5(NH_4)[HAsW_7O_{28}Os(dmso)_3]\cdot 15H_2O$ (**1a**)

As1–O15	1.663 (8)	As1–O22	1.724 (8)
As1–O28	1.663 (8)	As1–O1	1.663 (9)
W2–O5	1.903 (9)	W2–O6	2.278 (9)
W2–O7	1.732 (10)	W2–O8	1.728 (9)
W2–O9	1.940 (9)	W2–O10	2.187 (8)
W3–O10	2.175 (9)	W3–O9	1.936 (8)
W3–O11	1.741 (8)	W3–O12	1.756 (9)
W3–O13	1.906 (8)	W3–O14	2.286 (8)
W4–O13	1.991 (8)	W4–O14	2.207 (7)
W4–O15	2.252 (9)	W4–O16	1.898 (8)
W4–O17	1.735 (8)	W4–O18	1.728 (9)
Os1–O20	2.088 (9)	Os1–O23	2.068 (9)
Os1–O28	2.118 (8)	S1–O29	1.493 (9)
O30–S2	1.469 (10)	Os1–S2	2.238 (3)
O31–S3	1.493 (10)	Os1–S3	2.226 (3)
Os1–S1	2.233 (3)	Na1–O30	2.410 (11)
Na1–O33	2.404 (11)	Na1–O35	2.488 (12)
Na1–O32	2.407 (17)	Na2–O36	2.363 (12)
Na1–O17	2.539 (11)	Na2–O29	2.400 (11)
Na2–O35	2.317 (11)	Na2–O30	2.479 (12)
Na2–O37	2.398 (15)	Na3–O33	2.301 (12)
Na2–O31	2.413 (11)	Na3–O32	2.457 (16)
Na3–O29	2.242 (11)	Na4–O8	2.344 (10)
Na3–O36	2.460 (13)	Na4–O12	2.422 (11)
Na4–O18	2.407 (11)		
O28–As1–O1	109.8 (5)	O28–As1–O15	112.9 (5)
O15–As1–O22	107.7 (4)	O1–As1–O22	106.9 (4)
O28–As1–O22	110.3 (4)	O1–As1–O15	108.9 (5)
O8–W2–O7	102.3 (5)	O8–W2–O5	97.3 (4)
O8–W2–O6	166.6 (4)	O8–W2–O10	90.5 (4)
O8–W2–O9	101.8 (4)	O17–W4–O16	100.7 (4)
O18–W4–O17	102.1 (4)	O17–W4–O14	160.8 (4)
O17–W4–O13	94.3 (4)	O18–W4–O15	170.1 (4)
O17–W4–O15	87.7 (4)		

X-ray crystallography. X-ray single-crystal data for **1a** was set on the end of a glass capillary for indexing and intensity data collection at 293 K on the a Rigaku/MSC mercury diffractometer with graphite monochromated Mo$K\alpha$ radiation ($\lambda = 0.71073$ Å). Direct methods were used to solve the structures and to locate the heavy atoms (SHELXS97). Then the remaining atoms were found from successive difference maps (SHELXL97). All the non-hydrogen atoms were refined anisotropically. Further details of the X-ray structural analysis are given in Table 1. Selected bond lengths and angles are listed in Table 2.

3. Results and discussion

3.1. Synthesis and structure

The Os-supported tungstoarsenate $Na_5(NH_4)[HAsW_7O_{28}Os(dmso)_3]\cdot 15H_2O$ (**1a**) has been synthesized in good yield in a simple one-pot procedure by reaction of $[HAsW_9O_{34}]^{8-}$ with *cis*-Os(dmso)$_4$Cl$_2$ in aqueous medium (pH 6.0) and isolated as the sodium–ammonium salt. The polyoxoanion $[HAsW_7O_{28}Os(dmso)_3]^{6-}$ (**1**) consists of an Os(dmso)$_3$ group attached to a tungstoarsenate fragment resulting in an open assembly with C_s symmetry (Fig. 1). The Os(dmso)$_3$ unit is coordinated via two Os–O–W bonds and one Os–O–As bond to the polyanion backbone of **1**. The structure of the polyanion **1** is closely related to the Ru-supported tungstoarsenate $[HAsW_7O_{28}Ru(dmso)_3]^{6-}$ and the isostructural tungstophosphate $[HPW_7O_{28}Ru(dmso)_3]^{6-}$ [47].

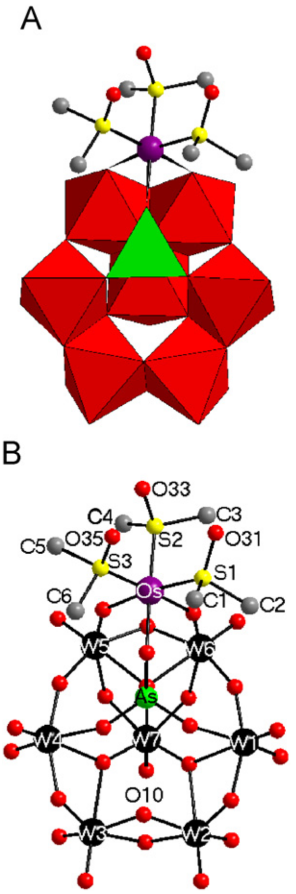

Fig. 1. (A) Combined polyhedral/ball and stick representation of $[HAsW_7O_{28}Os^{II}(dmso)_3]^{6-}$ (**1**). The WO$_6$ octahedra are red and the AsO$_4$ tetrahedron is green. The color code of the balls is: osmium (wine), sulfur (yellow), carbon (gray), and oxygen (red). Hydrogen atoms are omitted for clarity. (B) Ball and stick representation of the tungsten-oxo core of $[HAsW_7O_{28}Os^{II}(dmso)_3]^{6-}$ (**1**). The color code of the balls is: tungsten (black), arsenic (green), osmium (wine), sulfur (yellow), carbon (gray), and oxygen (red). Hydrogen atoms are omitted for clarity.

Polyanion **1** represents the first structurally characterized Os-supported polytungstate by single-crystal X-ray diffraction. There is only one report in the literature on Os(dmso)-supported polytungstate $[\alpha\text{-}PW_{11}O_{39}\{Os(dmso)_3(H_2O)\}]^{5-}$, but this species could only be characterized by IR, ^{1}H NMR, ^{31}P NMR, and DFT. In latter structure, Os(dmso)$_3$ unit is grafted to two nonequivalent oxygen atoms of the lacuna $[PW_{11}O_{39}]^{7-}$, which plays the bidentate role for this structure. However, in **1**, Os(dmso)$_3$ fragment is bound to three nonequivalent oxygen atoms of polyanion fragment $\{HAsW_7O_{28}\}$: two oxo-groups are from the tungsten-oxo framework and one is from the hetero group As–O. Such bonding of an (organo) Os fragment involving actively also the hetero group of the polyanion has never been observed before.

Recently, Neumann and co-workers reported the same Os(dmso)$_3$ fragment in the heptamolybdate polyanion $[Os(dmso)_3Mo_7O_{24}]^{4-}$ [44]. In this compound the osmium (II) center is coordinated to three oxo-groups of the molybdenum-oxo core and to the sulfur atoms of three terminal dmso ligands. In our structure the osmium (II) center is also coordinated to three oxo-groups from tungstoarsenate polyanion $\{HAsW_7O_{28}\}$ with the distances of 2.068–2.118 Å and three sulfur atoms from three terminal dmso ligands with the distances of 2.226–2.238 Å. The above results indicate that three of the originally four dmso ligands in *cis*-Os(dmso)$_4$Cl$_2$ appear to be rather strongly bound to the Os (II) center as they remain attached during synthesis of **1a** (which involved heating to 80 °C for 1 h in buffer solution). The same case has been observed for the Ru(dmso)-supported POMs [34,35,47].

Synthesis of **1** was performed by reaction of $[HAsW_9O_{34}]^{8-}$ with *cis*-Os(dmso)$_4$Cl$_2$ in about equimolar ratio in buffer solution (pH: 6.0). Therefore, the reaction mechanism must involve metal Os coordination and conversion of the trilacunary to the tungstoarsenate fragment ($\{HAsW_9O_{34}\}\rightarrow\{HAsW_7O_{28}\}$) following the loss of W$_2$O$_6$. Close inspection of **1** indicates that removal of the Os(dmso)$_3$ group would result in the hypothetical polyanion $\{HAsW_7O_{28}\}$, which is composed of one edge-shared W$_3$O$_{13}$ triad (W5, W6 and W7) and a half-ring of four edge-shared WO$_6$ octahedra (W1, W2, W3 and W4) and they are connected via corners and this assembly is stabilized by the central AsO$_4$ group. As a result, the three tungsten centers of the W$_3$O$_{13}$ triad have one terminal oxo ligand whereas the remaining four tungsten atoms have two, *cis*-related terminal oxo groups. The same observations are seen in $[HXW_7O_{28}Ru(dmso)_3]^{6-}$ ($X =$ P and As) [47]. However, we have not been able to isolate $\{HAsW_7O_{28}\}$ as an independent species yet, indicating that *cis*-M(dmso)$_4$Cl$_2$ ($M =$ Ru, Os) is essential for the formation of $\{HAsW_7O_{28}\}$.

In addition, polyanion **1** can also be synthesized from the source precursors of As$_2$O$_5$, Na$_2$WO$_4$ and *cis*-Os(dmso)$_4$Cl$_2$ by the mixture of all the chemicals in one pot under the same experimental condition as for the synthesis of **1a**, as based on the IR spectrum.

Bond valence sum (BVS) [48] calculations for **1** suggest that the μ_2-oxo group O10 bridging tungsten centers W2 and W3 (Fig. 1) is monoprotonated as the bond valence sum for O10 is $s = 0.98$ which is the value expected for a hydroxo group ($s = 1$). Therefore, the charge of the polyanion **1** must be -6. The -6 charge of **1** is balanced by one NH_4^+ and five Na$^+$ ions in the solid state. All counterions are distributed evenly around the polyanion and are bound to some of its terminal oxo ligands and water molecules of hydration as well as the oxo atoms of the three dmso molecules coordinated to osmium. Interestingly, three Na ions (Na1, Na2, Na3) form helix sodium chain which is composed of NaO$_6$

octahedra and NaO_5 square-pyramidal cone all sharing edges with their neighboring polyhedron (see Fig. 2). The polyanion **1** is distributed between the sodium chains and connected to the chains by the oxo atoms (W4–O17–Na1, S1–O29–Na2/Na3, S2–O30–Na1/Na2, S3–O31–Na2), leading to a 2D network-like structure (network-1, see Fig. 2). Moreover, the other sodium atoms Na4, Na5, and Na6 connected each other (Na4–O41–Na6, Na4–O40–Na5) by sharing the corner are linked to two polyanions **1** forming a unprecedented pseudosandwich-type tungstoarsenate functionalized by $Os(dmso)_3$ groups (Na4–O18–W4, Na4–O12–W3, Na5–O25–W6, Na5–O37–W7, Na6–O26–W7, Na6–O12–W3, Na6–O19–W5) (see Fig. 3A). In addition, the pseudosandwich-type tungstoarsenates further form 2D structure by the Na4–O8–W2 bond (network-2, see Fig. 3B). The other interesting feature is that network-1 and network-2 are connected each other to form the 3D structure by the Na atoms (see Fig. 4). According to our knowledge, such structure has never been observed for the Ru/Os-supported POMs so far and is rarely observed in the POMs chemistry.

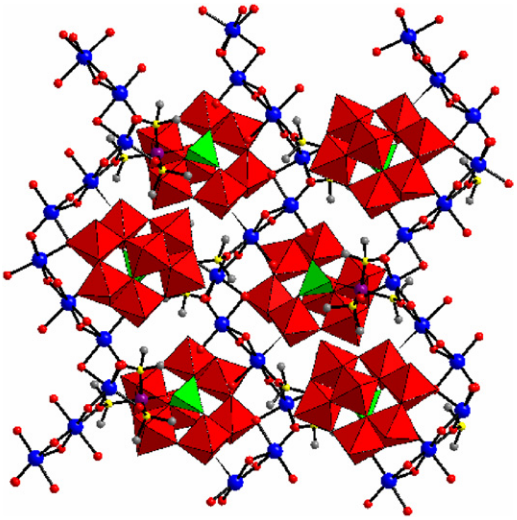

Fig. 2. Combined polyhedral/ball and stick representation of the 2D structure of compound **1a**. The color code is same as in Fig. 1. Hydrogen atoms, NH_4^+, Na4, Na5, Na6, and free water molecules are omitted for clarity.

3.2. NMR spectra

In order to determine the structures of **1a** further, we performed the multinuclear, room temperature NMR studies on **1a** redissolved in D_2O. As shown in Fig. 5, the ^{13}C-NMR and ^1H-NMR spectra of **1a** show three signals at 45.2, 45.8, and 46.0 ppm with ratio of 2:2:2 and 3.28, 3.35, and 3.45 ppm with a ratio of 6:6:6, respectively. This is in complete agreement with the structure of **1**, which indicates the presence of three types of carbon atoms (C1/C2, C3/C4, and C5/C6) and hydrogen atoms coordinated to the carbon atoms in **1a**. This means that all three dmso ligands in **1a** are magnetically inequivalent in solution, but

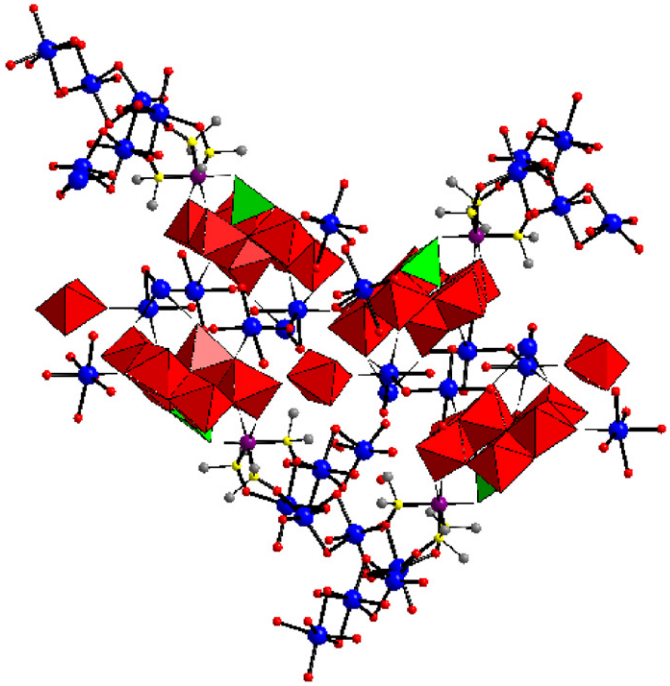

Fig. 4. Combined polyhedral/ball and stick representation of the 3D structure of compound **1a**. The color code is same as in Fig. 1. Hydrogen atoms, NH_4^+, and free water molecules are omitted for clarity.

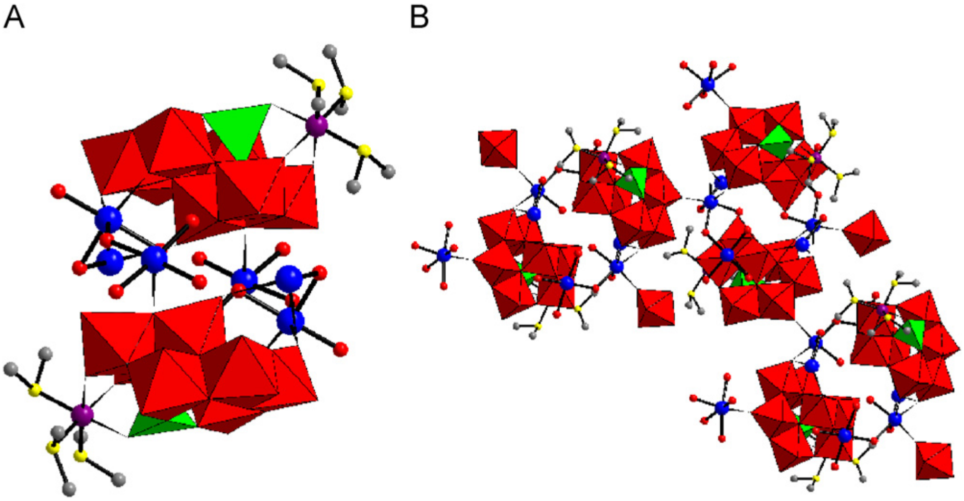

Fig. 3. (A) Combined polyhedral/ball and stick representation of pseudosandwich-type tungstoarsenate. (B) Combined polyhedral/ball and stick representation of the 2D structure of pseudosandwich-type tungstoarsenate. The color code is same as in Fig. 1. Hydrogen atoms, NH_4^+, Na1, Na2, Na3, and free water molecules are omitted for clarity.

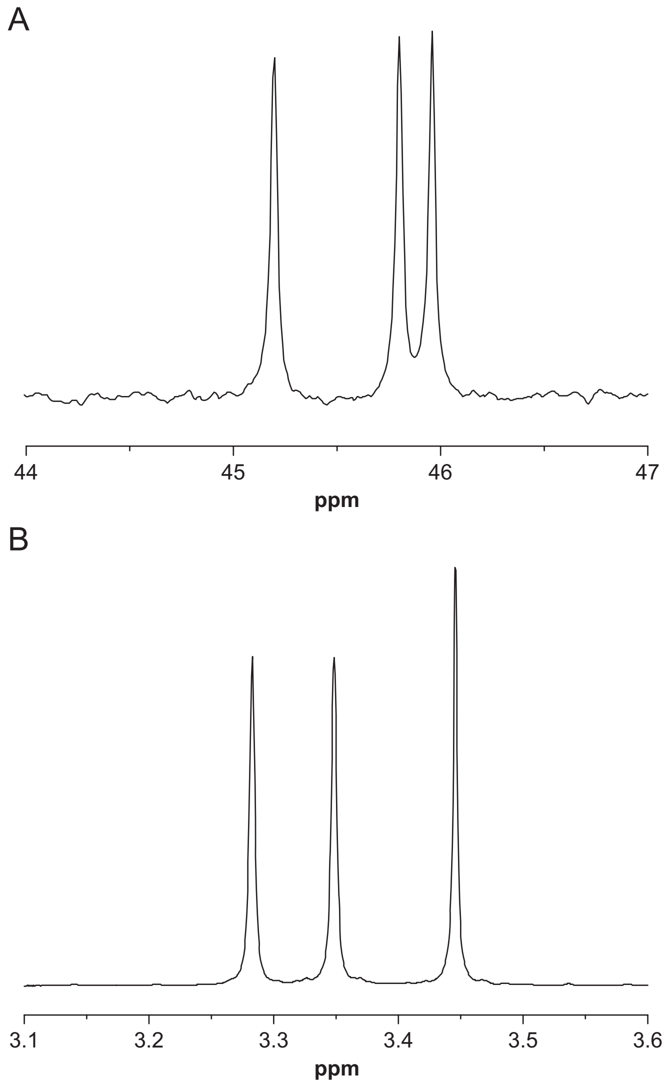

Fig. 5. (A) Room temperature ^{13}C NMR spectrum of $[HAsW_7O_{28}Os^{II}(dmso)_3]^{6-}$ (**1**) in D_2O. (B) Room temperature ^{1}H NMR spectrum of $[HAsW_7O_{28}Os^{II}(dmso)_3]^{6-}$ (**1**) in D_2O.

the two methyl groups within each dmso molecule are magnetically equivalent. The only reasonable explanation for this is hindered rotation of the dmso ligands around the Os–S bond. The same results have been observed in $[HXW_7O_{28}Ru(dmso)_3]^{6-}$ ($X = $ P and As) [47].

3.3. Cyclic voltammetry

To determine the redox properties of compound **1a**, we studied the electrochemical behavior of **1a** in the buffer solution. Fig. 6A shows the typical cyclic voltammetric behaviors of **1a** at scan rate 10 mV s^{-1} in the pH 2.0 (0.5 M Na_2SO_4+H_2SO_4) buffer solution. It can be seen that in the potential range 0.2 to−0.6 V on a GCE two redox peaks appear and the mean peak potentials $E_{1/2} = (E_{pa}+E_{pc})/2$ are −0.44 V (I–I′) and −0.53 V (II–II′) (vs Ag/AgCl), respectively. The two peaks I–I′ and II–II′ may be attribute to the redox of the $W^{VI/V}$ in the polyanion framework. The CVs of **1a** in same pH medium at different scan rates are shown in Fig. 6B. The peak currents of **1a** are linearly proportional to the square root of the scan rates, taking the oxidation I and the reduction peak II′ of **1a** as representative, as shown in the inset of Fig. 6B. This indicates that the redox processes are diffusion-controlled.

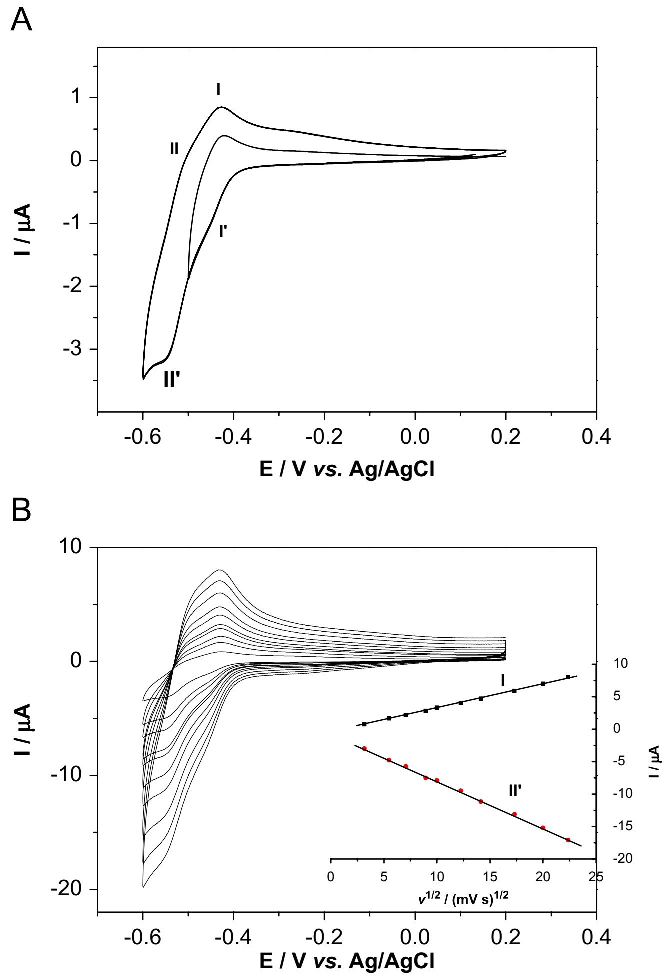

Fig. 6. (A) CVs of 1.0 mM **1a** in 0.5 M Na_2SO_4+H_2SO_4 at pH 2.0 with different potential limits: −0.5 and −0.6 V. Scan rate: 10 mV s^{-1}. (B) CVs of 1.0 mM **1a** in 0.5 M Na_2SO_4+H_2SO_4 at pH 2.0 at scan rates of 10, 30, 50, 80, 100, 150, 200, 300, 400, and 500 mV s^{-1}. The inset shows the relationship of the square root of scan rates vs. the oxidation peak currents I and reduction peak currents II′.

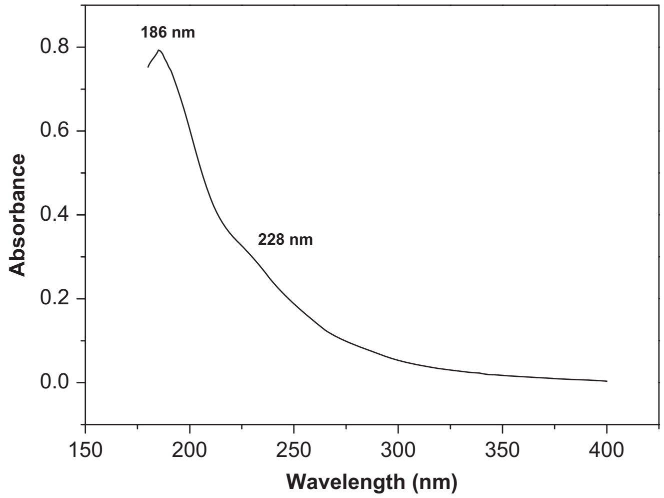

Fig. 7. UV–Vis electronic spectrum in aqueous solutions for **1a** within a range of 180–400 nm, 1.1 × 10^{-5} mol L^{-1} in ultraviolet region.

3.4. Electronic spectroscopy

The UV–Vis electronic spectrum of compound **1a** is displayed in Fig. 7. In the wavelength range between 180 and 400 nm the two strong absorption bands with maximum around 186 and 228 nm are observed. The peak at 186 nm is assigned to Od→W charge transition and the other peak at 228 nm is assigned to Ob(c)→W charge transition, which are the characteristic charge transfer bands from oxygen to tungsten in the POM framework.

4. Conclusions

In summary, we have synthesized and structurally characterized Os^{II}-supported tungstoarsenate for the first time. The novel polyanion $[HAsW_7O_{28}Os(dmso)_3]^{6-}$ (**1**) consists of a $Os(dmso)_3$ unit linked to a polyanion $\{HAsW_7O_{28}\}$fragment via two Os–O–W bonds and one Os–O–As bond resulting in an assembly with C_s symmetry. The solid state structure of **1a** consists of the polyanion **1** linked by Na^+ cations to constitute a 3D architecture.

Supporting information and structure details

Crystallographic data for the structure reported in this paper in the form of CIF file have been deposited with the ICSD team, FIZ Karlsruhe, Hermann-von-Helmholtz-Platz 1, D-76344 Eggenstein-Leopoldshafen (crysdata@fiz-karlsruhe.de) by quoting the depository number CSD 419761 (http://www.ccdc.cam.ac.uk/products/csd/deposit/).

Acknowledgment

The authors acknowledge the financial support of the State Key Laboratory of Inorganic Synthesis and Preparative Chemistry of Jilin University.

References

[1] C.L. Hill, Chem. Rev. 98 (1998) 1–389 (Special thematic issue on polyoxometalates).
[2] J.J. Borrás-Almenar, E. Coronado, A. Müller, M.T. Pope (Eds.), Polyoxometalate Molecular Science, Kluwer, Dordrecht, The Netherlands, 2004.
[3] H.L. Li, H. Sun, W. Qi, M. Xu, L.X. Wu, Angew. Chem. Int. Ed. 46 (2007) 1300.
[4] J. Berzelius, Pogg. Ann. 6 (1826) 369.
[5] A. Proust, R. Thouvenot, P. Gouzerh, Chem. Commun. 16 (2008) 1837.
[6] C.P. Pradeep, D.L. Long, G.N. Newton, Y.F. Song, L. Cronin, Angew. Chem. Int. Ed. 47 (2008) 4388.
[7] Y.F. Song, D.L. Long, L. Cronin, Angew. Chem. Int. Ed. 46 (2007) 3900.
[8] D.L. Long, E. Burkholder, L. Cronin, Chem. Soc. Rev. 36 (2007) 105.
[9] C.L. Hill, J. Mol. Catal. A-Chem. 262 (2007) 1.
[10] C. Qin, X.L. Wang, E.B. Wang, Z.M. Su, Inorg. Chem. 47 (2008) 5555.
[11] H. Liu, C. Qin, Y.G. Wei, L. Xu, G.G. Gao, F.Y. Li, X.S. Qu, Inorg. Chem. 47 (2008) 4166.
[12] G.G. Gao, L. Xu, X.S. Qu, H. Liu, Y.Y. Yang, Inorg. Chem. 47 (2008) 3402.
[13] A.X. Tian, J. Ying, J. Peng, J.Q. Sha, Z.G. Han, J.F. Ma, Z.M. Su, N.H.H.Q. Jia, Inorg. Chem. 47 (2008) 3274.
[14] R.G. Cao, S.X. Liu, L.H. Xie, Y.B. Pan, J.F. Cao, Y.H. Ren, L. Xu, Inorg. Chem. 46 (2007) 3541.
[15] W. Adam, P.L. Alsters, R. Neumann, C.R. Saha-Moller, D. Seebach, A.K. Beck, R. Zhang, J. Org. Chem. 68 (2003) 8222.
[16] W. Adam, P.L. Alsters, R. Neumann, C.R. Saha-Moller, D. Sloboda-Rozner, R. Zhang, J. Org. Chem. 68 (2003) 1721.
[17] V. Kogan, Z. Aizenshtat, R. Neumann, New J. Chem. 26 (2002) 272.
[18] R. Neumann, A.M. Khenkin, D. Juwiler, H. Miller, M.J. Gara, Mol. Catal. A-Chem. 117 (1997) 169.
[19] S.J. Angus-Dunne, R.C. Burns, D.C. Craig, G.A. Lawrance, J. Chem. Soc. Chem. Commun. (1994) 523.
[20] L.-H. Bi, M. Reicke, U. Kortz, B. Keita, L. Nadjo, R.J. Clark, Inorg. Chem. 43 (2004) 3915.
[21] L.-H. Bi, U. Kortz, B. Keita, L. Nadjo, H. Borrmann, Inorg. Chem. 43 (2004) 8367.
[22] L.-H. Bi, U. Kortz, B. Keita, L. Nadjo, L. Daniels, Eur. J. Inorg. Chem. 15 (2005) 3034.
[23] T.M. Anderson, W.A. Neiwert, M.L. Kirk, P.M.B. Piccoli, A.J. Schultz, T.F. Koetzle, D.G. Musaev, K. Morokuma, R. Cao, C.L. Hill, Science 306 (2004) 2074.
[24] T.M. Anderson, R. Cao, E. Slonkina, B. Hedman, K.O. Hodqson, K.I. Hardcastle, W.A. Neiwert, S.X. Wu, M.L. Kirk, S. Knottenbelt, E.C. Depperman, B. Keita, L. Nadjo, D.G. Musaev, K. Morokuma, C.L. Hill, J. Am. Soc. Chem. 127 (2005) 11948.
[25] U. Lee, H.-C. Joo, K.-M. Park, T. Ozeki, Acta Crystallogr. Sect. C 59 (2003) 152.
[26] U. Lee, H.-C. Joo, K.-M. Park, S.S. Mal, U. Kortz, B. Keita, L. Nadjo, Angew. Chem. Int. Ed. 47 (2008) 793.
[27] T. Naota, H. Takaya, S.-I. Murahashi, Chem. Rev. 98 (1998) 2599.
[28] Y.V. Geletii, B. Botar, P. Koeqerler, D.A. Hillesheim, D.G. Musaev, C.L. Hill, Angew. Chem. Int. Ed. 47 (2008) 3896.
[29] C.N. Kato, A. Shinohara, N. Moriya, K. Nomiya, Catal. Commun. 7 (2006) 413.
[30] R.G. Finke, C.X. Yin, Inorg. Chem. 44 (2005) 4175.
[31] R. Neumann, M. Dahan, J. Am. Chem. Soc. 120 (1998) 11969.
[32] R. Neumann, M. Dahan, Nature 388 (1997) 353.
[33] R. Neumann, A.M. Khenkin, M. Dahan, Angew. Chem. Int. Ed. Engl. 34 (1995) 1587.
[34] L.-H. Bi, F. Hussain, U. Kortz, M. Sadakane, M.H. Dickman, Chem. Commun. (2004) 1420.
[35] L.-H. Bi, U. Kortz, B. Keita, L. Nadjo, Dalton Trans. (2004) 3184.
[36] Y. Sakai, A. Shinohara, K. Hayashi, K. Nomiya, Eur. J. Inorg. Chem. 1 (2006) 163.
[37] V. Artero, D. Laurencin, R. Villanneau, R. Thouvenot, P. Herson, P. Gouzerh, A. Proust, Inorg. Chem. 44 (2005) 2826.
[38] D. Laurencin, R. Villanneau, P. Herson, R. Thouvenot, Y. Jeannin, A. Proust, Chem. Commun. (2005) 5524.
[39] L.-H. Bi, E.V. Chubarova, N.H. Nsouli, M.H. Dickman, U. Kortz, B. Keita, L. Nadjo, Inorg. Chem. 45 (2006) 8575.
[40] L.-H. Bi, U. Kortz, M.H. Dickman, B. Keita, L. Nadjo, Inorg. Chem. 44 (2005) 7485.
[41] L.K. Yan, Z. Don, W. Guan, S.Q. Shi, Z.M. Su, Eur. J. Inorg. Chem. 24 (2006) 5126.
[42] C. Dablemont, C.G. Hamaker, R. Thouvenot, Z. Sojka, M. Che, E.A. Maatta, A. Proust, Chem. A-Eur. J. 12 (2006) 9150.
[43] D. Laurencin, R. Villanneau, H. Gerard, A. Proust, J. Phys. Chem. A 110 (2006) 6345.
[44] A.M. Khenkin, L.J.W. Shimon, R. Neumann, Inorg. Chem. 42 (2003) 3331.
[45] L.H. Bi, R.D. Huang, J. Peng, E.B. Wang, Y.H. Wang, C.W. Hu, J. Chem. Soc. Dalton Trans. 2 (2001) 121.
[46] P.G. Antonov, Y.N. Kukushkin, V.I. Konnov, Y.P. Kostokov, Koord. Khim. 6 (1980) 1585.
[47] L.-H. Bi, M.H. Dickman, U. Kortz, I. Dix, Chem. Commun. (2005) 3962.
[48] I.D. Brown, D. Altermatt, Acta Cryst. B 41 (1985) 244.